

# Evolution of shell structure in neutron-rich calcium isotopes

G. Hagen,<sup>1,2</sup> M. Hjorth-Jensen,<sup>3,4</sup> G. R. Jansen,<sup>3</sup> R. Machleidt,<sup>5</sup> and T. Papenbrock<sup>2,1</sup>

<sup>1</sup>*Physics Division, Oak Ridge National Laboratory, Oak Ridge, TN 37831, USA*

<sup>2</sup>*Department of Physics and Astronomy, University of Tennessee, Knoxville, TN 37996, USA*

<sup>3</sup>*Department of Physics and Center of Mathematics for Applications, University of Oslo, N-0316 Oslo, Norway*

<sup>4</sup>*National Superconducting Cyclotron Laboratory and Department of Physics and Astronomy, Michigan State University, East Lansing, MI 48824, USA*

<sup>5</sup>*Department of Physics, University of Idaho, Moscow, ID 83844, USA*

We employ interactions from chiral effective field theory and compute the binding energies and low-lying excitations of calcium isotopes with the coupled-cluster method. Effects of three-nucleon forces are included phenomenologically as in-medium two-nucleon interactions, and the coupling to the particle continuum is taken into account using a Berggren basis. The computed ground-state energies and the low-lying  $J^\pi = 2^+$  states for the isotopes <sup>42,48,50,52</sup>Ca are in good agreement with data, and we predict the excitation energy of the first  $J^\pi = 2^+$  state in <sup>54</sup>Ca at 1.9 MeV, displaying only a weak sub-shell closure. In the odd-mass nuclei <sup>53,55,61</sup>Ca we find that the positive parity states deviate strongly from the naive shell model.

PACS numbers: 21.10.-k, 21.30.-x, 21.60.-n, 27.40.+z, 27.50.+e

*Introduction.* – The shell model is the paradigm for our understanding of atomic nuclei. Doubly magic nuclei (i.e., nuclei that exhibit an enhanced stability) are its cornerstones, and they determine the properties of nuclei in entire regions of the nuclear chart. The magic numbers – established *ad hoc* via a mean field plus a strong spin-orbit interaction more than 60 years ago by Mayer and Jensen for beta-stable nuclei [1] – are modified in neutron-rich nuclei, see for example Ref. [2] for a recent review. The magic nature of nuclei is reflected experimentally in enhanced neutron separation energies and a reduced quadrupole collectivity (i.e., a relatively high-lying first excited  $J^\pi = 2^+$  state and relatively small electromagnetic transition probabilities from this state to the  $J^\pi = 0^+$  ground state). In doubly magic nuclei such as <sup>40</sup>Ca and <sup>48</sup>Ca, the  $J^\pi = 2^+$  state appears at an excitation energy close to 4 MeV, while in open-shell calcium isotopes like <sup>42,44,46,50</sup>Ca, this excitation energy is closer to 1 MeV. How these quantities evolve as we move towards the driplines is an open issue in ongoing nuclear structure research and is intimately related to our fundamental understanding of shell evolution in nuclei.

For the theoretical understanding of shell evolution, phenomenological terms such as the tensor interaction [3] have been proposed. In a modern picture, three-nucleon forces (3NFs) play a pivotal role in shell evolution [4]. In the oxygen isotopes, for instance, 3NFs make <sup>24</sup>O doubly magic and a dripline nucleus [5–7]. Similarly, Holt *et al.* [8] showed that 3NFs are greatly responsible for the magic neutron number  $N = 28$ . On the other hand, experiment and theory show that the next possible magic number,  $N = 32$ , exhibits a smaller value for the  $2^+$  excitation (but more than twice as large as seen in open-shell calcium isotopes) than observed in <sup>48</sup>Ca. This is often referred to as a sub-shell closure. The  $N = 32$  sub-shell closure is well established from experiments in

calcium [9, 10], titanium [11], and chromium [12]. However, the situation is more complicated for neutron-rich calcium isotopes. For the neutron number  $N = 34$ , no sub-shell closure is seen experimentally in chromium [13] or titanium [14, 15], and there are some doubts regarding a sub-shell closure in calcium [16]. Different theoretical predictions have been made around  $N = 34$ . Within the *fp* shell-model space, the empirical interaction GXPF1 [17] predicts a strong shell gap in <sup>54</sup>Ca, while the monopole-corrected KB3 interaction [18] yields no shell gap. A low-momentum shell-model interaction with empirical single-particle energies and a <sup>48</sup>Ca core yields a weak sub-shell closure in <sup>54</sup>Ca [19]. Shell-model calculations that include 3NFs predict a shell closure in <sup>54</sup>Ca in the *fp* model space, and this shell closure is reduced to a sub-shell closure (similar in strength to the  $N = 32$  sub-shell closure in <sup>52</sup>Ca) in an enlarged model space that also includes the  $g_{9/2}$  orbital [8]. Thus, the picture regarding the shell gap in <sup>54</sup>Ca is not settled yet. The theoretical prediction of the shell evolution in calcium isotopes is a challenging task that requires a very good understanding of the nuclear interaction, accurate treatment of many-body correlations and coupling to the scattering continuum [20]. To study the shell evolution, we will focus on neutron separation energies, the energies of the first excited  $J^\pi = 2^+$  states, and spectra in the nuclei <sup>53,55,61</sup>Ca, which differ by one neutron from nuclei that exhibit a closed subshell in the naive shell model.

In this Letter, we present a state-of-the-art prediction for the shell evolution of neutron-rich calcium isotopes. To this purpose, we employ nucleon-nucleon ( $NN$ ) interactions from chiral effective field theory (EFT) together with a schematic approximation of 3NFs guided by chiral EFT, and utilize the coupled-cluster method to solve the quantum many-body problem. Chiral EFT is a system-

atic and model-independent approach to nuclear interactions. We employ the  $NN$  interactions at next-to-next-to-leading order by Entem and Machleidt [21, 22], and an approximation for the chiral 3NFs that was previously adopted in neutron-rich oxygen isotopes [7]. The coupled-cluster method [23, 24] is a very efficient tool for the computation of nuclei with a closed (sub-)shell structure and their neighbors, and thus ideally suited for the task at hand.

*Hamiltonian, model space, and method.* – We employ the intrinsic Hamiltonian

$$\hat{H} = \sum_{1 \leq i < j \leq A} \left( \frac{(\vec{p}_i - \vec{p}_j)^2}{2mA} + \hat{V}_{NN}^{(i,j)} + \hat{V}_{3\text{Neff}}^{(i,j)} \right). \quad (1)$$

Here, the intrinsic kinetic energy depends on the mass number  $A$ . The potential  $\hat{V}_{NN}$  denotes the chiral  $NN$  interaction at next-to-next-to-next-to-leading order [21, 22], while  $\hat{V}_{3\text{Neff}}$  is a schematic potential based on the in-medium chiral  $NN$  interaction by Holt *et al.* [25] (see also Ref. [26]). The potential  $\hat{V}_{3\text{Neff}}$  results from integrating one nucleon in the leading-order chiral 3NF over the Fermi sphere with Fermi momentum  $k_F$  in symmetric nuclear matter and is thus reminiscent of the normal-ordered approximation [27]. It depends formally on the Fermi momentum  $k_F$ , the low-energy constants  $c_D$  and  $c_E$  of the short-ranged contributions to the leading-order chiral 3NF, and the chiral cutoff. The latter is equal to the value employed in the chiral  $NN$  interaction [21]. In the computation of neutron-rich oxygen isotopes [7], the parameters  $k_F = 1.05 \text{ fm}^{-1}$  and  $c_E = 0.71$  resulted from adjusting the binding energies of  $^{16,22}\text{O}$ , while  $c_D = -0.2$  was kept at its value determined in light nuclei [28]. In this work, we use  $k_F = 0.95 \text{ fm}^{-1}$  and  $c_E = 0.735$  from adjusting the binding energies of  $^{48,52}\text{Ca}$ . It is very satisfying that the parameterization of  $\hat{V}_{3\text{Neff}}$  changes only little as one goes from neutron-rich isotopes of oxygen to the significantly heavier calcium isotopes.

The coupled-cluster method generates a similarity-transformed Hamiltonian  $\bar{H} = e^{-T} \hat{H} e^T$  by the action of the cluster operator  $T$  that creates up to  $n$ -particle- $n$ -hole ( $np$ - $nh$ ) excitations with respect to a reference state. Details of our implementation are presented in Refs. [29, 30]. We compute the ground states of the closed-(sub)shell nuclei  $^{40,48,52,54,60,62}\text{Ca}$  in the singles doubles (CCSD) approximation and include  $n = 3$  triples perturbatively within the  $\Lambda$ -CCSD(T) approach of Ref. [31]. Our model space consists of up to  $N_{\text{max}} = 19$  major spherical oscillator shells (i.e., the maximal single-particle excitation energy is 18 units of  $\hbar\omega$  above the oscillator ground state), and the reference state results from a Hartree-Fock calculation. Our basis employs oscillator spacings between  $24 \text{ MeV} \leq \hbar\omega \leq 32 \text{ MeV}$ , and in the largest model spaces the results we present are practically independent of  $\hbar\omega$ . For excited states in  $^{53,55,61}\text{Ca}$  above threshold, we use a Gamow-Hartree-Fock basis [7, 32]

with 40 discretization points [33]. Excited states of the closed-shell nuclei  $^{48,52,54}\text{Ca}$  are computed within the equation-of-motion (EOM) method with singles and doubles. The open-shell nuclei  $^{39,41,47,49,51,53,55,59,61}\text{Ca}$  are computed with the particle attached/removed EOM methods, and we use the two-particle attached EOM method [34] for the nuclei  $^{42,50,56}\text{Ca}$ . Note that the employed EOM methods are expected to reliably compute the separation energies and low-lying excited states as long as they are dominated by  $1p$ ,  $1h$ ,  $1p$ - $1h$  or  $2p$  excitations.

*Results.* – Figure 1 shows the computed ground-state energies of the calcium isotopes and compares the results obtained with the Hamiltonian of Eq. (1) to available data and to the results based on chiral  $NN$  interactions alone. The inclusion of chiral 3NFs via the in-medium effective potential  $\hat{V}_{3\text{Neff}}$  clearly yields a much improved agreement with data. The light isotopes  $^{39,40,41,42}\text{Ca}$  are slightly overbound, while the agreement is very good for the neutron-rich isotopes at the center of this study. The comparison with chiral  $NN$  forces shows that the in-medium effective potential  $\hat{V}_{3\text{Neff}}$  is repulsive [41]. For the heavier isotopes of calcium, the in-medium effective potential  $\hat{V}_{3\text{Neff}}$  becomes increasingly repulsive, and a saturation of the total binding energy sets in around  $^{60}\text{Ca}$ . It is interesting that essentially the same interaction yields attraction in neutron-rich oxygen isotopes [7]. Note that the results for the isotopes  $^{52-60}\text{Ca}$  are based on an exponential extrapolation of our results for  $N_{\text{max}} = 14, 16, 18$  oscillator shells at the oscillator frequency  $\hbar\omega = 26 \text{ MeV}$ . This extrapolation adds 0.6 MeV of binding energy in  $^{52}\text{Ca}$  and 1.2 MeV in  $^{60}\text{Ca}$ . For the other nuclei our results are practically converged with 19 shells. As a check, we also employed a Gamow Hartree-Fock basis for the  $s$ - $p$ - $d$  neutron partial waves and computed the ground states for the isotopes  $^{54,60}\text{Ca}$ . The differences are small (up to about 0.3 MeV) and barely noticeable on the scale of Fig. 1.

Figure 2 shows the energies of the  $J^\pi = 2^+$  states in the isotopes  $^{42,48,50,52,54,56}\text{Ca}$ , computed in a model space with  $N_{\text{max}} = 18$  and  $\hbar\omega = 26 \text{ MeV}$  for  $^{48,52,54}\text{Ca}$  and  $N_{\text{max}} = 16$  and  $\hbar\omega = 28 \text{ MeV}$  for  $^{42,50,56}\text{Ca}$ . Where data is available, we obtain a good agreement between theory and experiment. The 3NFs generate the shell closure in  $^{48}\text{Ca}$  and make  $N = 28$  a magic number. We also computed the  $J^\pi = 2^+$  excited state in  $^{48}\text{Ca}$  using chiral  $NN$  forces alone, and we obtained  $E_{2^+} = 2.07 \text{ MeV}$ ; this shows that the magicity of  $^{48}\text{Ca}$  is due to the effects of 3NFs in our approach. Our results predict that  $^{54}\text{Ca}$  exhibits only a weak sub-shell closure, and this is one of the main results of this Letter.

To further demonstrate this point, we also computed the energies of the first excited  $J^\pi = 4^+$  states, and neutron separation energies  $S_n$ . The results in Table I show that theory and experiment agree well for the available data. The theoretical results for  $^{54}\text{Ca}$  suggest strongly

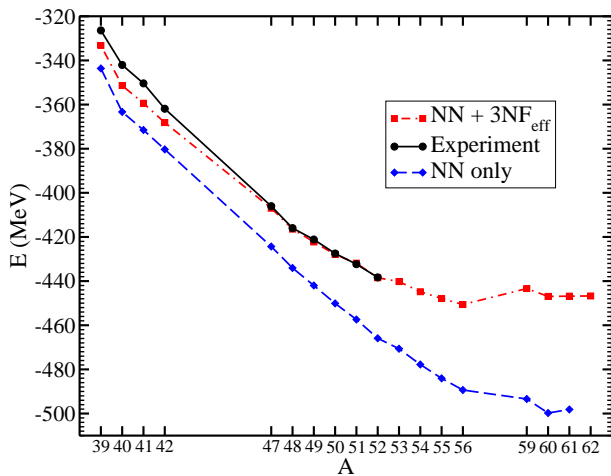


FIG. 1: (Color online) Ground-state energy of the calcium isotopes as a function of the mass number  $A$ . Black circles: experimental data; red squares: theoretical results including the effects of three-nucleon forces; blue diamonds: predictions from chiral  $NN$  forces alone. The experimental results for  $^{51,52}\text{Ca}$  are from Ref. [35].

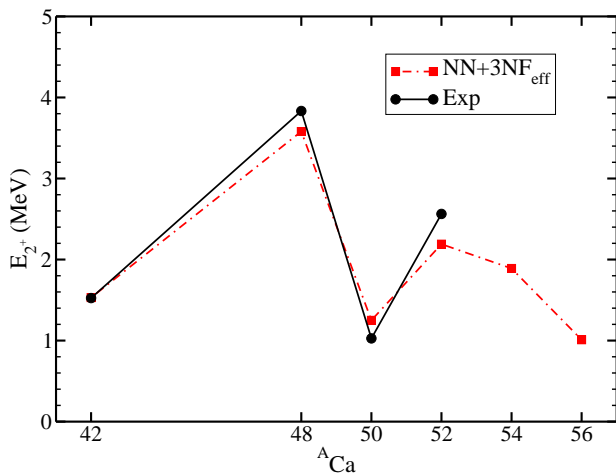


FIG. 2: (Color online) Excitation energies of  $J^\pi = 2^+$  states in the isotopes  $^{42,48,50,52,54,56}\text{Ca}$  (experiment: black, theory: red).

that this nucleus will only exhibit a weak sub-shell closure but not a shell closure. The neutron separation energy in  $^{52}\text{Ca}$  is a noteworthy example. The atomic mass table evaluation [36] gives the value  $S_n = 4.7$  MeV (estimated from systematics) for this nucleus. The very recent measurement [35], however, yields  $S_n \approx 6$  MeV, in much better agreement with our prediction of  $S_n = 6.59$  MeV.

To further study the evolution of shell structure we focus on spectra. Figure 3 shows the computed spectra for  $^{52-56}\text{Ca}$ , and compares them to available data. In  $^{52,53}\text{Ca}$ , our calculations suggest spin assignments for measured levels [37], while we give predictions for sev-

eral levels in  $^{52,53,54,55,56}\text{Ca}$ . The scattering continuum is shown as a gray band. Note that we computed the  $J^\pi = 2^+$  excited state of  $^{54}\text{Ca}$  as a  $1p-1h$  excitation of the  $^{54}\text{Ca}$  ground state and as  $2p$  excitations of the  $^{52}\text{Ca}$  ground state. In 17 major oscillator shells we obtain  $E_{2^+} = 1.80$  MeV and  $E_{2^+} = 1.90$  MeV, respectively. The two methods are in good agreement with each other, and this shows the quality of the employed methods.

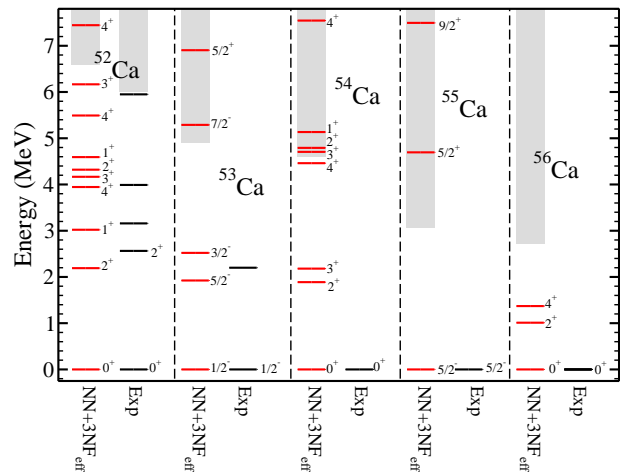


FIG. 3: (Color online) Theoretical excitation spectra of  $^{52-56}\text{Ca}$  compared to available data. The continuum is indicated as a gray area.

In the naive shell-model picture, the order of single-particle orbitals above the Fermi surface of  $^{60}\text{Ca}$  is  $g_{9/2}$ ,  $d_{5/2}$  and  $s_{1/2}$ . Mean-field calculations predict that the corresponding canonical orbitals are close in energy [38], yielding deformation in the isotopes  $^{60-70}\text{Ca}$  [39]. The isotope  $^{58}\text{Ca}$  is the heaviest isotope of calcium that has been produced [40], and  $^{52}\text{Ca}$  is the most neutron-rich isotope whose mass is known [35]. Nuclear energy functionals and mass models [38, 39] predict the neutron

	$^{48}\text{Ca}$	$^{52}\text{Ca}$	$^{54}\text{Ca}$
$E_{2^+}$ (CC)	3.58	2.19	1.89
$E_{2^+}$ (Exp)	3.83	2.56	n.a.
$E_{4^+}/E_{2^+}$ (CC)	1.17	1.80	2.36
$E_{4^+}/E_{2^+}$ (Exp)	1.17	n.a.	n.a.
$S_n$ (CC)	9.45	6.59	4.59
$S_n$ (Exp)	9.95	6.0*	4.0 <sup>†</sup>

TABLE I: Excitation energies  $E_{2^+}$  (in MeV) of the lowest-lying  $J^\pi = 2^+$  states, neutron-separation energies  $S_n$  (in MeV), and ratio of energies  $E_{4^+}/E_{2^+}$  from coupled-cluster theory (CC) compared to available data (Exp) [n.a. = not available; \* = from Ref. [35]; <sup>†</sup> = from atomic mass table evaluation [36]]. The theoretical results point to a sub-shell closure in  $^{54}\text{Ca}$ .

drip line to be around  $^{70}\text{Ca}$ . Figure 3 shows that the  $J^\pi = 5/2^+$  resonant excited states in  $^{53,55}\text{Ca}$  are lower in energy than the  $J^\pi = 9/2^+$  states, and this is a deviation from the naive shell-model picture. There is no  $J^\pi = 1/2^+$  resonance in the continuum due to absence of a centrifugal barrier. Due to the large  $l = 4$  centrifugal barrier the  $J^\pi = 9/2^+$  resonances can be considered as quasi-bound states, while the  $J^\pi = 5/2^+$  has a significantly larger width, see Table II for details. Our results shown in Fig. 1 yield  $^{60}\text{Ca}$  unbound with respect to  $^{56}\text{Ca}$ . However, we cannot rule out the existence of  $^{60}\text{Ca}$  since correlations beyond triples in the coupled-cluster expansion may play a larger role for  $^{60}\text{Ca}$  than for the neighbors of  $^{54}\text{Ca}$ . Our computations (including the scattering continuum) suggest that  $^{61}\text{Ca}$  is a very interesting nucleus. We find resonant states  $J^\pi = 5/2^+$  and  $J^\pi = 9/2^+$  at excitation energies of 1.1 MeV and 2.2 MeV above threshold, respectively, and a virtual  $J^\pi = 1/2^+$  state practically at threshold. This ordering of the resonances is consistent with the results for  $^{53,55}\text{Ca}$ . Table II summarizes our results for the  $J^\pi = 5/2^+$  and  $J^\pi = 9/2^+$  resonances in  $^{53,55,61}\text{Ca}$ . We also find the  $^{62}\text{Ca}$  ground state to be very close to threshold, unbound by about 0.2 MeV with respect to  $^{60}\text{Ca}$  and entirely dominated by  $(s_{1/2})^2$  configurations. In our calculations, the correct treatment of the continuum is essential: (i) in  $^{55}\text{Ca}$  the scattering continuum lowers the energy of the excited  $J^\pi = 5/2^+$  by about 2 MeV when compared to a harmonic oscillator basis, (ii) in  $^{61}\text{Ca}$ , the oscillator basis yields the level ordering of the naive shell model.

	$^{53}\text{Ca}$		$^{55}\text{Ca}$		$^{61}\text{Ca}$	
$J^\pi$	Re[E]	$\Gamma$	Re[E]	$\Gamma$	Re[E]	$\Gamma$
$5/2^+$	1.99	1.97	1.63	1.33	1.14	0.62
$9/2^+$	4.75	0.28	4.43	0.23	2.19	0.02

TABLE II: Energies of the  $5/2^+$  and  $9/2^+$  resonances in  $^{53,55,61}\text{Ca}$ . Re[E] is the energy relative to the one-neutron emission threshold, and the width is  $\Gamma = -2\text{Im}[E]$  (in MeV).

As a check, we also computed the lowest excited states with spin and parity  $J^\pi = 2^+, 4^+, 6^+$  in  $^{50,54,56}\text{Ti}$ . These states result from attaching two protons to the closed-core reference nuclei  $^{48,52,54}\text{Ca}$ , respectively, and we employ  $2p-0h$  and  $3p-1h$  excitations in the computation. Figure 4 shows a reasonably good agreement with the data, with a maximal deviation of about 0.6 MeV for the  $2_1^+$  state in  $^{56}\text{Ti}$ . Let us compare the titanium isotopes to the isotopes  $^{50,54,56}\text{Ca}$  which might also be computed by attaching two neutrons to  $^{48,52,54}\text{Ca}$ , respectively. The analysis of the cluster amplitudes shows that the  $2p-0h$  cluster amplitudes account for about 60% of the total amplitude for the isotopes of titanium, while this number is about 72% for the calcium isotopes (with the remaining weight carried by  $3p-1h$  amplitudes). It is insightful to compare the ratios of  $3p-2h$  to  $2p-0h$  amplitudes.

These are about 0.67 in titaniums and only 0.39 in calciums. Thus, the isotopes of titanium are more correlated due to proton-neutron interactions than the corresponding calcium isotopes. We believe that one needs  $4p-2h$  amplitudes for a more accurate description.

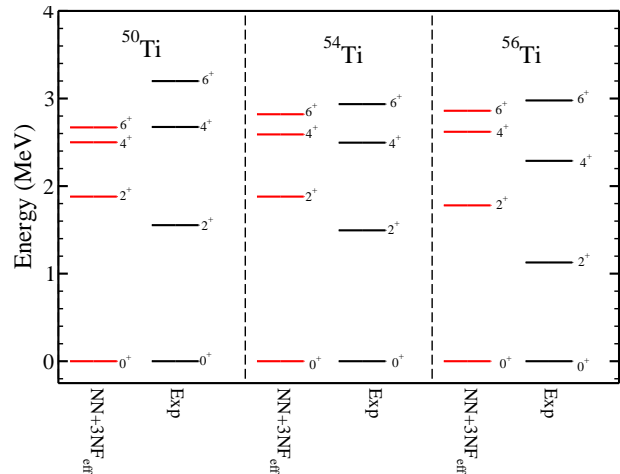


FIG. 4: (Color online) Theoretical excitation spectra of  $^{50,54,56}\text{Ti}$  compared to data.

*Summary.* – We employed interactions from chiral effective field theory and performed coupled-cluster computations of neutron-rich calcium isotopes. The evolution of shell structure is understood by our computations of neutron-separation energies, low-lying  $J^\pi = 2^+, 4^+$  states, and excitations in the odd-mass nuclei  $^{53,55,61}\text{Ca}$ . Our results confirm that the shell closure in  $^{48}\text{Ca}$  is due to the effects of three-nucleon forces, and that  $^{52}\text{Ca}$  exhibits a sub-shell closure while  $^{54}\text{Ca}$  exhibits only a weak sub-shell closure. We make several predictions for spin and parity assignments in the spectra of very neutron-rich isotopes of calcium and predict a level ordering in  $^{53,55,61}\text{Ca}$  that is at variance with the naive shell model. Overall, we find that effects of three-nucleon forces and the scattering continuum are essential in understanding the evolution of shell structure towards the dripline.

We acknowledge valuable discussions with S. K. Bogner, B. A. Brown, R. J. Furnstahl, K. Hebeler, J. D. Holt, W. Nazarewicz, and A. Schwenk. This work was supported by the Office of Nuclear Physics, U.S. Department of Energy (Oak Ridge National Laboratory). This work was supported in part by the U.S. Department of Energy under Grant Nos. DE-FG02-03ER41270 (University of Idaho), DE-FG02-96ER40963 (University of Tennessee), and DE-FC02-07ER41457 (UNEDF SciDAC). This research used computational resources of the National Center for Computational Sciences, the National Institute for Computational Sciences, and the Notur project in Norway.

- 
- [1] M. Mayer and J. H. D. Jensen, *Elementary Theory of Nuclear Shell Structure*, Wiley, New York (1955).
- [2] O. Sorlin and M.-G. Porquet, *Prog. Part. Nucl. Phys.* **61**, 602 (2008).
- [3] T. Otsuka *et al.*, *Phys. Rev. Lett.* **95**, 232502 (2005)
- [4] A. P. Zuker, *Phys. Rev. Lett.* **90**, 042502 (2003).
- [5] T. Otsuka *et al.*, *Phys. Rev. Lett.* **105**, 032501 (2010).
- [6] J. D. Holt and A. Schwenk, arxiv:1108:2680 (2011).
- [7] G. Hagen *et al.*, *Phys. Rev. Lett.* **108**, in press (2012) and arXiv:1202.2839 (2012).
- [8] J. D. Holt *et al.*, arXiv:1009.5984v2 (2011).
- [9] A. Huck *et al.*, *Phys. Rev. C* **31**, 2226 (1985).
- [10] A. Gade *et al.*, *Phys. Rev. C* **74**, 021302 (2006).
- [11] R. V. F. Janssens *et al.*, *Phys. Lett. B* **546**, 55 (2002).
- [12] J. I. Prisciandaro *et al.*, *Phys. Lett. B* **510**, 17 (2001).
- [13] N. Marginean *et al.*, *Phys. Lett. B* **633**, 696 (2006)
- [14] S. N. Liddick *et al.*, *Phys. Rev. Lett.* **92**, 072502 (2004).
- [15] D.-C. Dinca *et al.*, *Phys. Rev. C* **71**, 041302 (2005).
- [16] M. Rejmund *et al.*, *Phys. Rev. C* **76**, 021304 (2007).
- [17] M. Honma *et al.*, *Phys. Rev. C* **65**, 061301 (2002).
- [18] E. Caurier *et al.*, *Rev. Mod. Phys.* **77**, 427 (2005).
- [19] L. Coraggio *et al.*, *Phys. Rev. C* **80**, 044311 (2009).
- [20] J. Dobaczewski *et al.*, *Prog. Part. Nucl. Phys.* **59**, 432 (2007).
- [21] D. R. Entem and R. Machleidt, *Phys. Rev. C* **68**, 041001(R) (2003).
- [22] R. Machleidt and D. R. Entem, *Phys. Rep.* **503**, 1 (2011).
- [23] F. Coester, *Nucl. Phys.* **7**, 421 (1958); F. Coester and H. Kümmel, *Nucl. Phys.* **17**, 477 (1960); J. Čížek, *J. Chem. Phys.* **45**, 4256 (1966); J. Čížek, *Adv. Chem. Phys.* **14**, 35 (1969); H. Kümmel, K.H. Lührmann, and J.G. Zabolitzky, *Phys. Rep.* **36**, 1 (1978).
- [24] R. J. Bartlett and M. Musiał, *Rev. Mod. Phys.* **79**, 291 (2007).
- [25] J. W. Holt, N. Kaiser, and W. Weise, *Phys. Rev. C* **79**, 054331 (2009); *ibid.* *Phys. Rev. C* **81**, 024002 (2010).
- [26] K. Hebeler and A. Schwenk, *Phys. Rev. C* **82**, 014314 (2010); K. Hebeler *et al.*, *Phys. Rev. C* **83**, 031301 (2011).
- [27] G. Hagen *et al.*, *Phys. Rev. C* **76**, 034302 (2007).
- [28] D. Gazit, S. Quaglioni, and P. Navrátil, *Phys. Rev. Lett.* **103**, 102502 (2009).
- [29] G. Hagen *et al.*, *Phys. Rev. Lett.* **101**, 092502 (2008).
- [30] G. Hagen *et al.*, *Phys. Rev. C* **82**, 034330 (2010).
- [31] A. D. Taube and R. J. Bartlett, *J. Chem. Phys.* **128**, 044110 (2008); *ibid.* **128**, 044111 (2008).
- [32] N. Michel *et al.*, *J. Phys. G* **36**, 013101 (2009).
- [33] G. Hagen and J. S. Vaagen, *Phys. Rev. C.* **73**, 064307 (2006).
- [34] G. R. Jansen *et al.*, *Phys. Rev. C.* **83**, 054306 (2011).
- [35] A. Lapierre *et al.*, *Phys. Rev. C* **85**, 024317 (2012); A. T. Gallant *et al.*, arXiv:1204.1987 (2012).
- [36] G. Audi, A. H. Wapstra, and C. Thibault, *Nucl. Phys. A* **729**, 337 (2003).
- [37] F. Perrot *et al.*, *Phys. Rev. C* **74**, 014313 (2005).
- [38] J. Meng *et al.*, *Phys. Rev. C* **65**, 041302 (2002); S. A. Fayans, S. V. Tolokonnikov, and D. Zawischa, *Phys. Lett. B* **491**, 245 (2000).
- [39] W. Nazarewicz *et al.*, *Phys. Rev. C* **53**, 740 (1996); J. Erler *et al.*, to be published (2012).
- [40] O. B. Tarasov *et al.*, *Phys. Rev. Lett.* **102**, 142501 (2009); O. B. Tarasov, private communication (2012).
- [41] The binding energy of  $^{40,48}\text{Ca}$  resulting from chiral  $NN$  interactions alone is larger than previously reported in Refs. [29, 30]. In the present work we use a higher cutoff ( $J_{\text{max}} = 10$ ) in the relative angular momentum when transforming the  $NN$  interaction from the center-of-mass frame to the laboratory frame.